Chapter 3

Species delimitations in the *Dicranum acutifolium* complex (Dicranaceae, Bryophyta) using molecular markers

A. S. Lang D. Tubanova & M. Stech

Journal of Bryology, in press

ABSTRACT

Because of their morphological plasticity and broad geographic distribution, the taxonomy of *Dicranum* is difficult. The circumscription of the different species included in the *Dicranum acutifolium* complex is poorly understood and taxonomic confusions are frequent. The present study extends earlier ITS-based phylogenetic reconstructions of the *D. acutifolium* complex by analysing five additional chloroplast markers (*trnT-rps4, trnL-F, psbA-trnH, rps19-rpl2, rpoB*) together with ITS of a larger taxon sampling. The phylogenetic analyses delimit *Dicranum acutifolium* (Lindb. & Arnell) C.E.O Jensen, *D. bardunovii* Tubanova & Ignatova, *D. brevifolium* (Lindb.) Lindb., and *D. septentrionale* Tubanova & Ignatova, which together form the *D. acutifolium* complex, and confirm that *D. pseudoacutifolium* is synonymous with *D. flexicaule*. *Dicranum septentrionale* was known so far from across Russia but also occurs in Scandinavia, where it was probably overlooked due to morphological resemblance with *D. brevifolium*. The problem of mixed collections for identification is exemplified by the holotype of *D. bardunovii*, which contains also individuals of the morphologically most similar *D. acutifolium* according to the molecular data. Morphometric analyses support the differentiation of the *D. acutifolium* complex. Furthermore, ordination analyses point to a continuous range of variation among species within the *D. acutifolium* complex, especially due to the larger variation of *D. septentrionale*.

INTRODUCTION

Dicranum Hedw. (including *Orthodicranum* (Bruch & Schimp.) Loeske) is a large moss genus of more than 90 accepted species (Frey & Stech 2009; Tropicos.org) with a predominantly Holarctic distribution. Several *Dicranum* species are known to be morphologically plastic (Hedenäs & Bisang 2004; Ireland 2007), and their circumscriptions remain ambiguous as neither a thorough worldwide revision nor a complete phylogenetic analysis of *Dicranum* is available yet. Nevertheless, a number of recent studies tackled certain groups of *Dicranum* species based on molecular data, namely

the *D. scoparium* Hedw. complex (Lang & Stech 2014), arctic *Dicranum* species (Lang *et al*. 2014), *Dicranum* species with fragile leaves (Ignatova & Fedosov, 2008) or the *D. acutifolium* (Lindb. & Arnell) C.E.O. Jensen and *D. fuscescens* Turner complexes (Tubanova *et al*. 2010; Tubanova & Ignatova 2011). The former two studies concluded that (closely related) *Dicranum* species can be best delimited based on combined analysis of five chloroplast markers and the nuclear ribosomal ITS region. Inferences on the *D. acutifolium* complex, in contrast, were based on ITS only and need to be re-evaluated based on a larger marker sampling.

The *Dicranum acutifolium* complex is part of *Dicranum* sect. *Spuria* Bruch & Schimp. (sensu Nyholm, 1987) and centred around two circumarctic – alpine species, *D. acutifolium* and *D. brevifolium* (Lindb.) Lindb. They were first described as varieties of *D. bergeri* Blandow (Lindberg & Arnell 1890) or *D. muehlenbeckii* Bruch & Schimp. (Lindberg 1865), respectively, the former being an erroneous name for *D. undulatum* (cf. Hedenäs & Bisang 2004). Otnyukova (2007) described a new species, *D. pseudoacutifolium* Otnyukova, which differed from *D. acutifolium* and *D. brevifolium* in morphological characters such as the absence of bulgings above cell walls, non-porose lower leaf cells, and inner perichaetial leaves abruptly contracted into a subula. However, molecular data revealed that the type specimen of this species corresponded to a weak form of *D. flexicaule* Brid., with whom it has been consequently synonymized (Tubanova *et al*. 2010), while other *D. pseudoacutifolium* specimens had identical ITS sequences with *D. acutifolium* (Tubanova *et al*. 2010). On the other hand, two newly identified molecular lineages were described as species, i.e. *D. septentrionale* Tubanova & Ignatova and *D. bardunovii* Tubanova & Ignatova (Tubanova *et al*. 2010; Tubanova & Ignatova 2011). These two species are morphologically very close to *D. brevifolium*, but also share several features with *D. acutifolium*. However, neither the newly described species nor *D. brevifolium* or *D. acutifolium* formed strongly supported clades based on ITS sequences only. The *Dicranum acutifolium* complex, in line with Tubanova *et al*. (2010), thus comprises four species, *D. acutifolium*, *D. brevifolium*, *D. bardunovii* and *D. septentrionale*. It is characterised by a combination of morphological characters including leaves that are keeled distally with the blade shaped like a pair of tongs in cross-section as well as thick-walled lamina cells that are subquadrate to short rectangular, sometimes irregularly shaped above and elongated and porose below.

This study extends the phylogenetic reconstructions of Tubanova *et al*. (2010) and Tubanova & Ignatova (2011) by analysing five chloroplast markers (*trnT-rps4, trnL-F, psbA-trnH, rps19-rpl2, rpoB*) in combination with ITS of a larger taxon sampling. Based on the molecular data and a re-evaluation of morphological characters, we aim to (i) add further molecular support to the circumscription of the *D. acutifolium* complex, (ii) clarify species circumscriptions in the complex, and in particular evaluate the taxonomic status of *D. bardunovii* and *D. septentrionale*, and (iii) investigate the value of morphological characters used to distinguish the species of the complex.

Materials and Methods

Sampling— A total of 67 *Dicranum* specimens were sampled (Appendix 1). The sampling included 15 specimens of which ITS sequences had already been generated by Tubanova *et al*. (2010) and Tubanova & Ignatova (2011), 12 specimens newly sequenced for all six markers employed here (see below), and 40 specimens of which chloroplast and ITS sequences were generated for previous studies (Lang & Stech 2014; Lang *et al*. 2014; Stech, 1999; Stech *et al*. 2006). We studied 29 specimens of sect. *Spuria*: six originally identified as *D. acutifolium,* 13 *D. brevifolium,* two *D. septentrionale*, three *D. bardunovii* (including the holotype, from which two

plants were sequenced separately), one *D. drummondii,* and four *D. undulatum*. Eight *Dicranum* species were included as representatives of other sections than sect. *Spuria*: four specimens of *D. spadiceum* J.E. Zetterst. (sect. *Muehlenbeckia* Peterson), three *D. elongatum* Schleich. ex Schwägr. (sect. *Elongata* Hag.), five *D. fuscescens* and 11 D. *flexicaule* (sect. *Fuscescentiformia* Kindb.), seven *D. majus* Turner, two *D. nipponense* Besch., two *D. scoparium*, and three *D. bonjeanii* De Not. (all sect. *Dicranum* Hedw.). *Dicranum muehlenbeckii* (sect. *Muehlenbeckia*) could not be included in the molecular analyses because of unsuccessful DNA amplification. However, two specimens were included in the morphological analyses. Previous studies resolved *Holomitrium* Brid. as sister group of *Dicranum* (La Farge *et al*. 2002; Stech *et al*. 2006). Therefore, four samples, one *H. crispulum* Mart. and three *H. arboreum* Mitt., were chosen as outgroup representatives (Appendix 1).

DNA extraction, amplification and sequencing— The greenest part of single gametophyte shoots was selected for DNA extraction. After cleaning the shoot under a binocular, total DNA was extracted using the NucleoSpin® Extract II Kit (Macherey-Nagel, Düren, Germany). Six markers employed to delimit closely related *Dicranum* species in Lang & Stech (2014) and Lang *et al*. (2014) were amplified and sequenced: five chloroplast regions (partial *rpoB* gene, $trnH_{GUG}$-*psbA*, *rps19-rpl2*, and *rps4-*$trnT_{UGU}$ intergenic spacers, and $trnL_{UAA}$ intron / $trnL_{UAA}$-$trnF_{GAA}$ intergenic spacer) and the nuclear ribosomal nrITS1-5.8S-ITS2 region. PCR amplifications were performed as described in Lang & Stech (2014). All PCR products were purified and sequenced at Macrogen Inc. (www.macrogen.com). GenBank accession numbers of all sequences are listed in Appendix 1.

Alignment and phylogenetic reconstruction— Alignment and phylogenetic reconstruction

Sequences were aligned in Geneious v6.1.6 (Biomatters, available from www.geneious.com) using 65% similarity matrix costs, and manually adjusted. One short hairpin-associated inversion in the *trnH-psbA* spacer, which can flip at the population level and may significantly reduce phylogenetic structure if undetected (Quandt & Stech 2004; Borsch & Quandt 2009; Whitlock *et al*. 2010), was positionally separated in the alignment and not coded as indels.

The best substitution model was selected for each locus according to the Akaike information criterion (AIC) using MrModeltest (Posada & Crandall, 1998) executed through PAUP* 4.0b10 (Swofford 2002). Gaps were coded as informative by simple indel coding (SIC) (Simmons & Ochoterena 2000) as implemented in SeqState (Müller 2004). To check for incongruence, phylogenetic reconstructions based on chloroplast and nuclear sequences were visually compared. In addition, an incongruence length difference test (ILD, Farris *et al*. 1994) as implemented in PAUP* was performed with 100 replicates. As both visual inspections and the ILD test indicated that the plastid and nuclear tree topologies were congruent (p=0.03), the two datasets were combined for analysis in a total evidence approach.

Phylogenetic inferences were based on maximum parsimony (MP), maximum likelihood (ML) and Bayesian inference (BI) analyses, with and without indels coded by SIC included. Heuristic searches under parsimony were performed in PAUP* using simple sequence addition with 1000 replicates and tree bisection-reconnection (TBR) branch swapping. The nucleotide matrix was divided into three partitions for ML and BI, namely the non-coding chloroplast markers (*rps4-trnT*, *trnL-trnF*, *trnH-psbA*, *rps19-rpl2*), the chloroplast gene *rpoB*, and the nrITS region. Maximum likelihood analyses were carried out with RAxML v.7.2.6 (Stamatakis 2006) employing the graphical user interface raxmlGUI v.0.93 (Silvestro & Michalak 2012). As implemented in RAxML, the GTR model

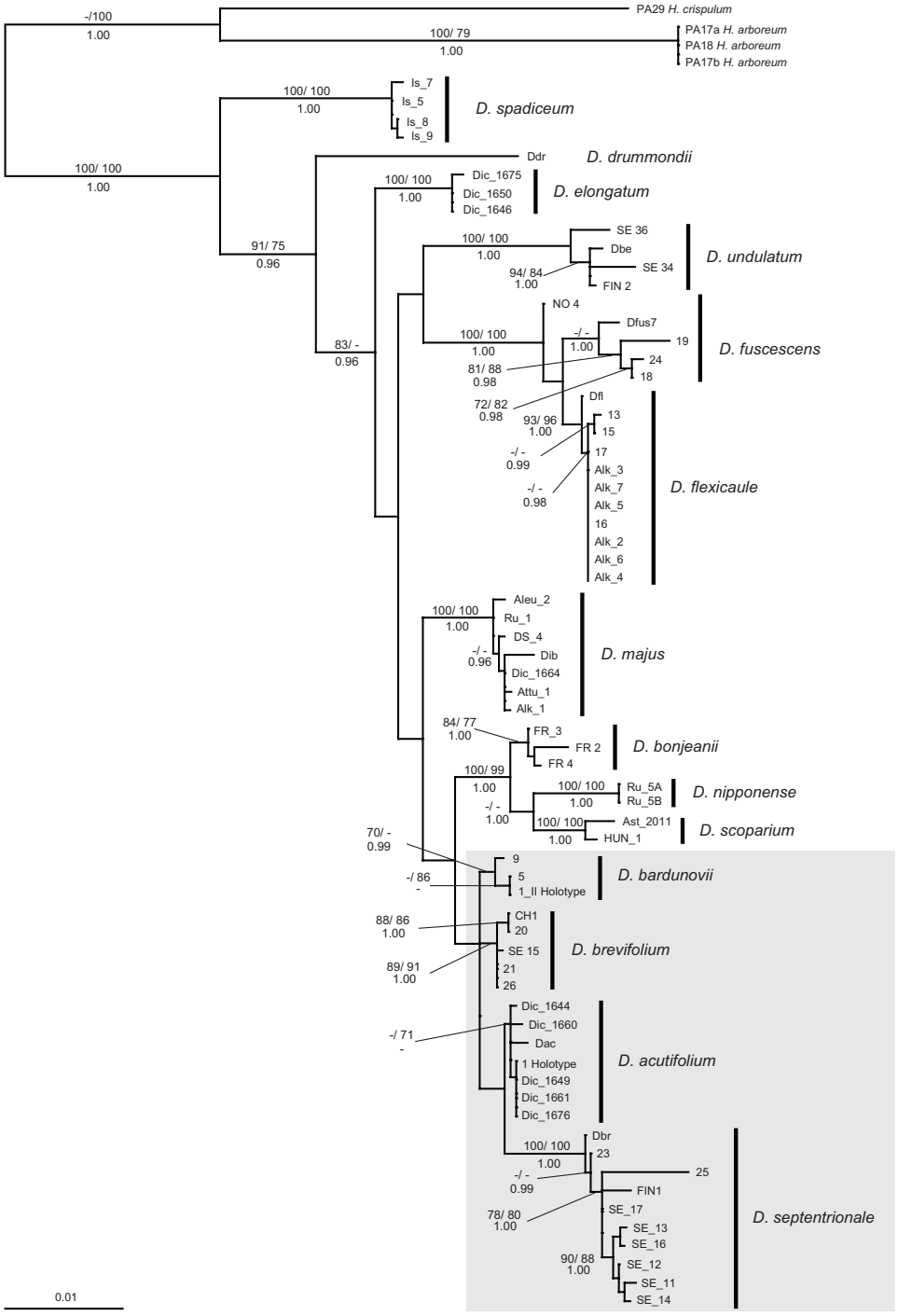
PA29 H. crispulum
PA17a H. arboreum
PA18 H. arboreum
PA17b H. arboreum
Is_7
Is_5
Is_8
Is_9
D. spadiceum
Ddr
D. drummondii
Dic_1675
Dic_1650
Dic_1646
D. elongatum
SE 36
Dbe
SE 34
FIN 2
D. undulatum
NO 4
Dfus7
19
24
18
D. fuscescens
Dfl
13
15
17
Alk_3
Alk_7
Alk_5
16
Alk_2
Alk_6
Alk_4
D. flexicaule
Aleu_2
Ru_1
DS_4
Dib
Dic_1664
Attu_1
Alk_1
D. majus
FR_3
FR 2
FR 4
D. bonjeanii
Ru_5A
Ru_5B
D. nipponense
Ast_2011
HUN_1
D. scoparium
9
5
1_II Holotype
D. bardunovii
CH1
20
SE 15
21
26
D. brevifolium
Dic_1644
Dic_1660
Dac
1 Holotype
Dic_1649
Dic_1661
Dic_1676
D. acutifolium
Dbr
23
25
FIN1
SE_17
SE_13
SE_16
SE_12
SE_11
SE_14
D. septentrionale
0.01

of nucleotide substitution with Γ model of rate heterogeneity was used for all partitions. Bootstrap searches under ML were done using the thorough bootstrap heuristics algorithm with 20 runs and 1000 replicates. Bayesian analyses were run on the CIPRES science gateway (Miller *et al*. 2010). Bayesian posterior probabilities were calculated based on the Markov chain Monte Carlo (MCMC) method, using MrBayes v3.2.1 x64 (Huelsenbeck & Ronquist 2001; Ronquist & Huelsenbeck 2003), with MrModeltest best fit models HKY + Γ for the non-coding chloroplast markers and HKY + I for *rpoB* and nrITS. Nucleotide and indel data were treated as separate and unlinked partitions, employing the restriction site model ('F81') for the indel matrix as recommended by Ronquist *et al*. (2005). The a priori probabilities supplied were those specified in the default settings of the program. Two runs with four chains were run simultaneously (11×10^6 generations), with the temperature of the single heated chain set to 0.5. Chains were sampled every 1000 generations and the respective trees written to a tree file. Fifty percent majority rule consensus trees and posterior probabilities of clades were calculated by combining the four runs and using the trees sampled after the chains converged. Trace plots generated in Tracer v1.5 (Rambaut & Drummond 2007) were used to check for convergence of the runs (plateaus of all runs at comparable likelihoods) and to infer the 'burnin', which was set to 25%.

Morphological analysis— A total of 47 specimens were included in the morphological analyses: all six *D. acutifolium*, five *D. brevifolium*, three *D. bardunovii* and ten *D. septentrionale* as well as two *D. scoparium*, two *D. nipponense*, three *D. bonjeanii*, three *D. majus*, four *D. undulatum* and the four *D. spadiceum*, plus three additional *D. drummondii* and two *D. muehlenbeckii* specimens that could not be sequenced. Thirty-four gametophytic characters were scored according to their relevance for species identification (Nyholm, 1987; Hedenäs & Bisang 2004; Tubanova *et al*. 2010). As none of the examined samples carried sporophytes, sporophytic characters were not included in the statistical analyses. Presence or absence of character states was scored for each sample (Appendix 2). Morphological scoring was made under a light microscope on three branch leaves removed from the upper part of the stem, excluding the uppermost part. Three additional leaves were removed and used for scoring characters of costa cross-section. Multistate characters were artificially separated into binary characters for analytical reasons.

A multivariate approach was used to investigate the phenotypic affinities between the taxa of the *D. acutifolium* complex and other putatively closely related species. Morphological discontinuities were first explored through a hierarchical cluster analysis based on Jaccard distances and the complete-linkage method as clustering strategy using the vegan package (Oksanen *et al*. 2013) in R 2.15 (R Development Core Team 2013). Pearson's correlation coefficient was calculated to evaluate the optimal number of clusters. To further explore the morphological similarity of species, we performed an ordination with nonmetric multidimensional scaling (NMDS; Kruskal 1964) applying the metaMDS function of vegan with its default arguments. We used the Jaccard matrix to produce a five dimensional ordination (i.e., $k=5$) and plotted against species

◄— Fig. 1. Single optimal maximum likelihood phylogenetic reconstruction inferred from the partitioned matrix for the non-coding chloroplast loci(trnT-rps4- trnL-F- trnH-psbA- rps19- rpl2), the coding region *rpo*B and nrITS, including indels coded by simple indel coding (SIC). The default GTR+ Γ model was applied for all DNA partitions and F81 was employed for the indel matrix. Bootstrap analyses under ML were done using the thorough bootstrap heuristics algorithm with 20 runs and 1000 replicates. BI was obtained with the best fit models HKY + Γ for the first partition, and HKY + I for rpoB and nrITS and F81 for the indel matrix, after 11,000,000 generations with two runs and four chains and the temperature of the single heated chain set to 0.5. Trees were sampled every 1000 generations and a burnin was set to 25%. Four specimens of Holomitrium were used as outgroup representatives. Support values (MP and ML BS ≥70%, BI PP ≥0.95) are indicated at the branches. Grey boxes delimit species of the D. acutifolium complex.

groups. Differences between and among groups of the ordinations were tested using an analysis of similarities (ANOSIM; Clarke 1993; Chapman & Underwood 1999).

Results

The total chloroplast alignment comprised 1901 positions, of which 122 were variable, and 90 of the variable characters were parsimony-informative. Of the 1077 positions in the ITS alignment, 124 ambiguous positions were removed from the subsequent calculations. The remaining 953 positions comprised 160 variable characters, of which 113 were parsimony-informative. Simple indel coding of the combined dataset yielded 155 additional characters (excluding three corresponding to an inversion in *psbA-trnH*), of which 99 were parsimony-informative.

Similar consistency indices resulted from the most parsimonious phylogenetic reconstructions with and without indels included (CI 0.7206 versus 0.7386), indicating a slightly lower amount of homoplasy in the indel characters. The single optimal ML tree of the combined markers is shown in Fig. 1, with bootstrap support values (≥70% BS) from the parsimony and likelihood analyses as well as posterior probabilities (PP ≥95) from Bayesian inference indicated on the branches.

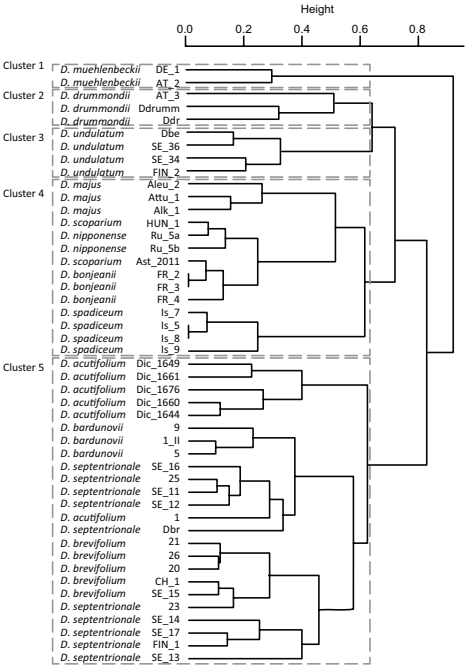

Fig. 2. Cluster dendrogram of 34 morphological characters and 47 specimens of *D. acutifolium*, *D. brevifolium*, *D. bardunovii*, *D. septentrionale*, *D. scoparium*, *D. bonjeanii*, *D. nipponense*, *D. majus*, *D. spadiceum*, *D. drummondii*, *D. muehlenbeckii* and *D. undulatum*, based on a Jaccard distance matrix and complete-linkage clustering strategy. The optimal number of clusters (k=5), delimited by the dashed rectangles, was calculated based on Pearson's correlation coefficient (r=0.769). Species names are based on the clades resolved in the molecular phylogenetic reconstructions.

Regardless of the phylogenetic inference, *D. brevifolium* and *D. septentrionale* were resolved in well-supported clades (≥89% BS, PP 1; Fig. 1). *Dicranum bardunovii* was less strongly supported (70% ML BS, PP 0.99), whereas *D. acutifolium* only received 71% BS in the ML analysis. Relationships among these four lineages remained ambiguous. *Dicranum drummondii*, which shares common morphological characters with species of the *D. acutifolium* complex, was clearly separated from the latter as well as from *D. undulatum* (100% BS, PP 1). One of the two plants of the holotype of *D. bardunovii* corresponded to *D. acutifolium*. Furthermore, eight of the 13 samples identified as *D. brevifolium* corresponded to *D. septentrionale* and only five were attributed to *D. brevifolium*. These confusions were due to mis-identifications of the samples, as the species are readily confused morphologically.

The *D. acutifolium* complex was resolved as sister group to the *D. scoparium* complex, but relationships between these two complexes as well as *D. majus*, *D. elongatum* and the *D. fuscescens* complex (*D. flexicaule* and *D. fuscescens*) remained unsupported.

The cluster analysis of morphological characters (Fig. 2) divided the analysed specimens

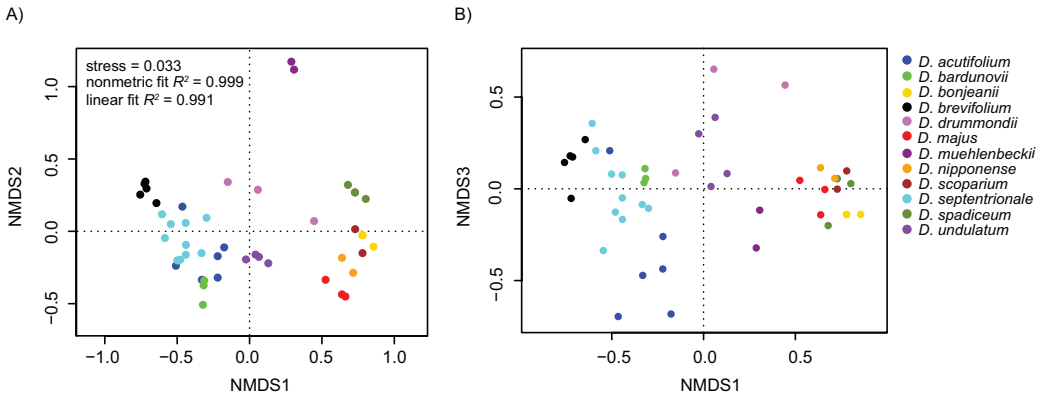

FIG. 3. Nonmetric Multidimensional Scaling (NMDS) ordinations of 47 *Dicranum* specimens using a Jaccard distance matrix and applying the metaMDS fonction of vegan with its default arguments (k=5). Scatterplots are showing the first and second (A), and first and third (B) dimensions. Species names are based on the clades resolved in the molecular phylogenetic reconstructions

into five optimal clusters (Pearson' s correlation coefficient r=0.769). *Dicranum muehlenbeckii*, *D. drummondii* and *D. undulatum* were grouped in clusters 1, 2 and 3, respectively. Cluster 4 included all the specimens of the *D. scoparium* complex plus *D. majus* and *D. spadiceum,* while all four species from the *D. acutifolium* complex grouped in cluster 5. Within the cluster of the *D. acutifolium* complex, three subclusters corresponded to *D. acutifolium*, *D. bardunovii* and *D. brevifolium*, respectively, whereas *D. septentrionale* did not form a homogeneous group, in contrast to the molecular tree. SE_11, SE_12, SE_16 and 25 formed a group that was most similar to *D. bardunovii*, SE_13, SE_14, SE_17, and FIN_1 formed a group that was most similar to *D. brevifolium* and one sample (23) clustered with *D. brevifolium*. Furthermore, both samples from the holotype of *D. bardunovii* (1 and 1_II) were situated in different subclusters, but sample 1 was not part of the *D. acutifolium* cluster, in contrast to the molecular tree.

The five clusters identified in the cluster analysis were best distinguishable by the first three axes of the NMDS scatterplot (Fig. 3; stress value= 0.033, nonmetric fit R^2=0.999, linear fit R^2=0.991). While the specimens included in the *D. acutifolium* complex formed a first group with negative values on axis one, the specimens of the *D. scoparium* complex, plus *D. spadiceum* and *D. majus* formed a second group with positive values. *Dicranum undulatum,* as well as *D. muehlenbeckii* and *D. drummondii,* was plotted between group one and two, with the former in the vicinity of group one. While axis two further allowed a clear distinction of *D. muehlenbeckii* (Fig. 3A), axis 3 confirmed the separation of *D. undulatum* from the *D. acutifolium* complex and the distinction of *D. brevifolium*, *D. acutifolium*, *D. bardunovii* (Fig. 3B). Although *D. septentrionale* was differentiated by axis 1 and 2, its similarity with *D. brevifolium* and *D. bardunovii* was displayed by axis 3. The differentiation among species was supported by the ANOSIM (R= 0.8867; p=0.001, 999 permutations).

DISCUSSION

Both the present molecular phylogenetic reconstructions (Fig. 1) as well as the morphological analyses (Fig. 2) support the current circumscription of the *D. acutifolium* species complex, which comprises *D. acutifolium*, *D. bardunovii*, *D. brevifolium*, and *D. septentrionale*. Morphologically

TABLE 1. Table of characters for D. acutifolium, D. brevifolium, D. septentrionale and D. bardunovii based on the present study and the literature (Tubanova et al. 2010; Tubanova& Ignatova, 2011).

	Leaf orientation	Leaf margin	Leaf apex	Alar cells	Lamina	Basal lamina cells	Median lamina cells	Upper lamina cells	Costa
D. acutifolium	Generally straight or slightly secund, slightly flexuose when dry. Not undulate.	Unistratose, entire.	Acuminate, serrulate, shaped like a pair of tongs in the middle and keeled to circular in apex.	Golden, bistratose.	Unistratose, no projecting cells, incrassate walls.	Rectangular to linear, not sharply different from median cells, porose,.	Quadrate to elongated, generally porose.	Irregularly arranged, irregualrely quadrate or elongated, generally eporose.	One row of guide cells, differentiated dorsal epidermis, smooth.
D. brevifolium	Generally secund, curled or twisted when dry. Not or slightly undulate in distal half.	Unistratose, occasionally bistratose in apex with geminate teeth	Acuminate, serrulate, shaped like a pair of tongs.	Golden, bistratose	Occasionally projecting cells in upper part, bulging cell walls, incrassate.	Rectangular, different from median cells, generally eporose.	Quadrate, eporose.	Regularly arranged, quadrate, eporose.	One row of guide cells, differentiated dorsal epidermis, with rugosity on the abaxial side.
D. septentrionale	Falcate secund, sometimes undulate, strongly curled when dry.	Unistratose, occasionally bistratose in apex with geminate teeth, serrulate.	Acuminate, serrulate, shaped like a pair of tongs, generally keeled in apex.	Generally golden, sometimes hyaline, bistratose.	Unistratose, occasionally with strongly projecting cells, especially in apex, bulging cell walls, incrassate.	Rectangular to linear, not sharply different form median cells, porose.	Quadrate to elongated, generally eporose.	Regularly arranged, irregularely quadrate, eporose.	One row of guide cells, sometimes with duplicated cells, differentiated dorsal epidermis, generally smooth.
D. bardunovii	Generally straight or slightly secund, slightly undulate, slightly flexuose when dry.	Unistratose, serrulate. occasionally bistratose in apex with geminate teeth	Acuminate, serrate, mostly shaped like a pair of tongs, generally keeled in apex.	Hyaline, bistratose.	Unistratose, with projecting cells, bulging cell walls, incrassate.	Generally rectangular, porose.	Quadrate to elongated, porose or not.	Regularly arranged, irregularely quadrate, projecting cells in upper half, eporose.	One row of guide cells, differentiated dorsal epidermis, projecting cells in upper half.

all four species together are characterised by incrassate lamina cells that are parenchymatous in the upper half of the leaf, acuminate and serrulate to serrate leaf apices, and a keeled upper leaf with incurved margins, resulting in a tong-shaped transverse section. The molecular data furthermore supports the conclusion of Tubanova *et al*. (2010) that *D. pseudoacutifolium* is synonymous with *D. flexicaule* (samples 13 and 15 in Fig. 1). Although supraspecific relationships in *Dicranum* remain largely unsupported based on the present molecular data (cf. also Lang & Stech 2014), and molecular relationships of *D. muehlenbeckii* await further study, no close relationship of the *D. acutifolium* complex with the other included species of sect. *Spuria*, *D. drummondii* and *D. undulatum*, nor with *D. fuscescens* (Fig. 1) and *D. muehlenbeckii* (Figs. 2, 3) are indicated. The latter two species share certain morphological characters with *D. acutifolium* and *D. brevifolium*, such as bulging cell walls, quadrate apical cells and slightly porose basal cells (e.g. Nyholm 1954, 1987; Ireland 2002), but are easily differentiated from the species of the *D. acutifolium* complex by their leaves not tong–shaped in cross section, thin lamina cell walls, and leaf margins serrate in the distal half. Despite its larger size, keeled leaf and the absence of bulging cell walls, *D. drummondii* is sometimes confused with *D. acutifolium* because of its flexuose leaves in dry state and irregularly shaped upper lamina cells (Ireland 2007; Nyholm 1987). *Dicranum undulatum* and *D. acutifolium* have both straight leaves that have projecting upper cells at back. However, the former has transversely undulate leaves that narrow into an obtuse apex, whereas the leaves of *D. acutifolium* end in a subulate point.

The existence of numerous intergrading forms occurring among the species of the *D. acutifolium* complex has caused much taxonomic confusion and led to frequent misidentifications. Their distinction is based on few subtle gametophytic characters (Table 1), and deviating forms render morphological identification difficult (Ireland 2002, 2007) as exemplified by the sample 1 of *D. acutifolium* or 23 of *D. septentrionale* (Figures 2, 3). Furthermore, herbarium collections of *D. brevifolium* were frequently found under different names, such as *D. drummondii*, *D. flexicaule*, or *D. undulatum* (Ireland 2002, Tubanova *et al*. 2010; Tubanova & Ignatova 2011). At the molecular level *D. acutifolium*, *D. bardunovii, D. brevifolium* and *D. septentrionale* seem more clearly distinguishable (Fig. 1), although the respective clades receive different statistical support, with *D. brevifolium* and *D. septentrionale* being well supported in all analyses, whereas *D. acutifolium* and *D. bardunovii* receive (lower) support only in part of the analyses. The molecular data also helped renaming misidentified specimens within the *D. acutifolium* complex, since a number of specimens identified as *D. brevifolium* were resolved in the clade of the *D. septentrionale* (Fig. 1). *Dicranum septentrionale* is a recently described species defined by few characters that were previously attributed to the morphological variation of *D. brevifolium* (Table 1). Nonetheless, the morphological characters frequently intergrade with *D. bardunovii* or *D. brevifolium* (Fig. 2, 3). According to the present results, *D. brevifolium* is characterised morphologically by tong-like leaf apices, elongated basal cells that are well differenciated from the median one and generally not porose, quadrate upper cells and rugose dorsal surface of the costa. In contrast, *D. septentrionale* is best differentiated by projecting lamina cells, especially at the leaf apex, elongated basal cell that gradually become quadrate, and irregularly shaped in the upper part of the leaf and a generally smooth dorsal epidermis. Furthermore, the distributions and ecological preferences of both *D. brevifolium* and *D. septentrionale* are incompletely known or misunderstood, considering that further *D. brevifolium* collections may appear to belong to *D. septentrionale*. While *D. septentrionale* was known so far from across Russia (Fig. 4), our study shows that its distribution range extends to

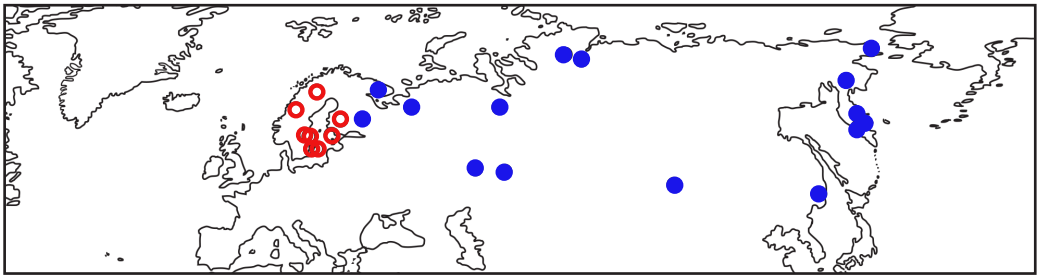

FIG. 4. Geographical distribution of *Dicranum septentrionale* according to collections studied in Tubanova et al. (2010) (filled blue dots) and the present study (empty red dots).

Scandinavia. This indicates that *D. septentrionale* has a Eurasian or possibly Holarctic distribution. In addition, the herbarium material we examined suggests that *D. septentrionale* could be a boreo-montane species, whereas *D. brevifolium* would be a (sub)arctic-alpine species, as suggested by previous studies (Amann *et al.* 1918; Dierssen 2001). A morpho-molecular re-identification of further specimens, including *D. brevifolium* from North America, is needed to delimit the distribution patterns and ecological preferences of *D. brevifolium* and *D. septentrionale* with more confidence.

Another part of the confusion between the species of the *D. acutifolium* complex may stem from the presence of mixed collections. A striking example is the holotype of *D. bardunovii*, which contains also individuals of the morphologically most similar *D. acutifolium* according to the molecular data (samples 1 and 1_II, Fig. 1). Not only are the morphological differences between *D. acutifolium* and *D. bardunovii* small (Table 1, Figs. 2-3), *D. bardunovii* also shows morphological variation departing from the holotype description. This is the case in the sequenced specimen 1, which resembles *D. septentrionale* by the presence of projecting cells in the lamina, the coloured alar cells and non porose, quadrate to elongated median lamina cells. Morphologically similar species growing in mixed cushions is not uncommon in *Dicranum*. For example, collections containing *D. scoparium* and *D. bonjeanii* have been found in locations where both species occurred also separately (own observations). Environmental conditions have a strong influence on morphological characters, especially in extreme conditions (Hedenäs *et al.* 2006), altering also typical characters. The distinction of closely related species is then even more difficult. Additionally, dwarf males growing on female stems (pseudomonoicy) are found both in *D. brevifolium* and *D. acutifolium* and have been seen in one *D. bardunovii* specimens (Tubanova & Ignatova 2011) a number of morphologically distinct specimens were revealed. They are similar to D. acutifolium (Lindb. & Arnell. Whether hybridisation, a process that affects also the morphology, occurs in mixed patches is still unknown. The present molecular data do not indicate any hybridisation for *D. acutifolium* and *D. bardunovii*, however, the absence of support for the *D. acutifolium* complex suggest that such a process might have occurred. The use of other molecular methods and more variable markers could be useful to understand the species dynamics at population level.

In line with a number of recent studies (e.g. Sukkharak *et al.* 2011; Carter 2012; Medina *et al.* 2012; Stech *et al.* 2013; Lang & Stech 2014) the present study displays the importance of molecular data for clarifying species circumscriptions, resolving taxonomical issues and for the re-evaluation of morphological characters in bryophytes and *Dicranum* in particular.